Stabilization of Proteins by Ligand Binding: Application to Drug Screening and Determination of Unfolding Energetics†

Travis T. Waldron and Kenneth P. Murphy*

Department of Biochemistry, Roy J. and Lucille A. Carver College of Medicine, University of Iowa, Iowa City, Iowa 52242

Received February 6, 2003; Revised Manuscript Received March 13, 2003

ABSTRACT: The observed stability of a protein is altered when ligands bind, which results in a shift in the melting temperature (T_m). Binding to the native state in the absence of binding to the denatured state will necessarily lead to an increase in the T_m, while binding to the unfolded state in the absence of native state binding will decrease the T_m relative to that of the protein in the absence of ligand. These effects are required by the thermodynamics of reversible folding. However, the relationship between binding affinity and the magnitude of the observed temperature shift is not a simple correlation (i.e., a larger shift in T_m does not necessarily mean tighter binding) and is complicated by interaction with the denatured state. Using exact simulations, the range of behavior for the dependence of the observed T_m shift on the energetics of ligand binding is investigated here. Specifically, differential scanning calorimetry (DSC) curves are simulated for protein unfolding in the presence of ligands binding to both the native and denatured states. The results have implications for drug screening and the determination of heat capacity changes for protein unfolding.

Binding to the native state of a protein in the absence of binding to the denatured state always stabilizes the native state. This is observed experimentally as an increase in the melting temperature (T_m)[1] of the protein in the presence of ligand, and this observable can be exploited as a drug screening method. By thermally denaturing a protein target in the absence and presence of various candidate ligands, one can quickly identify potential drugs that produce an increase in the melting temperature relative to that of the unliganded protein. Using the unfolding energetics in the absence of a ligand and the observed shift in T_m when a ligand is present, the binding constant for the interaction at the T_m can be calculated (*1*). However, when two or more ligands are compared, comparison of the calculated binding affinities requires extrapolation to a common temperature. It is easiest to extrapolate a short distance to the T_m of the protein in the presence of one of the ligands, where propagation errors in the energetics of protein unfolding are minimized, but if one ligand has a higher binding affinity at that T_m, it does not mean that this ligand has a higher binding affinity at a physiologically relevant temperature. Extrapolation to a physiologically relevant temperature requires that the energetics of ligand binding (enthalpy and heat capacity), as well as the energetics for unfolding in the absence of ligand (enthalpy and heat capacity), be known accurately.

Thermodynamic and statistical mechanical approaches to describing macromolecular unfolding linked to binding of a ligand have been discussed for some time (*2*, *3*). More recent discussions addressing the theory and its application to differential scanning calorimetry have also been presented (*1*, *4*−*6*). We have performed simulations for a number of related cases that differ from the previous approaches in several respects. First, and most importantly, the energetics of ligand binding are considered explicitly and are shown to have significant consequences. Previous treatments have assumed a binding enthalpy of zero since the binding enthalpy is small relative to the unfolding enthalpy. Second, we have included the equilibria for ligands binding to both the unfolded and native states. Finally, we avoid unnecessary approximations involving the concentration of free ligand (or the buffering capacity in the case of protons), since iterative techniques can determine these parameters with extremely high precision.

The results presented here are independent of the method used to monitor the unfolding event. We have chosen to focus on the use of differential scanning calorimetry (DSC) in monitoring protein unfolding in the presence of ligands since it has the potential to determine binding constants over a wide range of affinities (*1*), as well as the ability to fully characterize the energetics of binding and unfolding. We have simulated heat capacity curves for a variety of cases to demonstrate the relationships between the energetics of ligand binding and the observed melting temperature shifts. Given the need to accurately determine the unfolding

† This work was funded by the National Science Foundation (Grant MCB-9808073). T.T.W. was supported by an NIH fellowship to the Center for Biocatalysis and Bioprocessing at the Univeristy of Iowa.

* To whom correspondence should be addressed. E-mail: k-murphy@uiowa.edu.

[1] Abbreviations: T_m, melting temperature; T_o, melting temperature of a protein in the absence of ligand; K_u, equilibrium constant for the two-state protein unfolding process; $K_{a,i}$, intrinsic association constant for binding to the native state of the protein; $K_{b,j}$, intrinsic association constant for binding to the unfolded state of the protein; [X], free ligand concentration; ΔH_m, enthalpy for protein unfolding at the melting temperature; $\Delta C_{p,u}$, intrinsic heat capacity change for protein unfolding; DSC, differential scanning calorimetry; Q, partition function for states of a macromolecule; $\langle \Delta H \rangle$, excess enthalpy; $\langle \Delta C_p \rangle$, excess heat capacity; $[\text{ligand}]_{tot}$, total ligand concentration; $[\text{protein}]_{tot}$, total protein concentration; $[\text{buffer}]_{tot}$, total buffer concentration.

10.1021/bi034212v CCC: $25.00
Published on Web 04/11/2003

Scheme 1: Linkage Relations Considered in This Work[a]

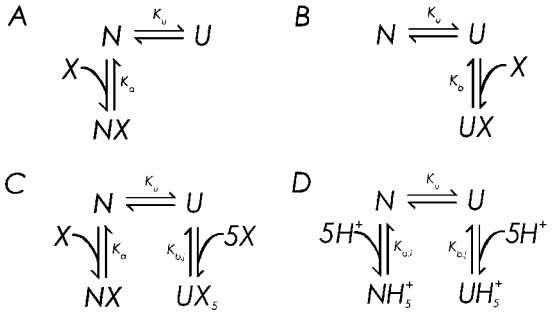

[a] (A) A single ligand binding to the native state. (B) A single ligand binding to the unfolded state. (C) A single ligand binding to the native state, with several bindings to the unfolded state. (D) Five bindings to both states, such as in the case of multiple proton binding sites with different affinities in the native and unfolded states.

energetics, we also studied the case of proton binding which has direct implications for the determination of heat capacity from plots of unfolding enthalpy versus melting temperature.

THEORY

The models discussed here are presented in Scheme 1, where panel D is the most general. The model allows for protein unfolding in the presence of any combination of binding events to the native and unfolded states of the protein. Binding equilibria are considered independent, but this assumption does not limit the generality of the conclusions. Included here are the cases of single-site binding to the native state (A) or the denatured state (B), as well as multiple-site binding to both states of the protein (C and D).

The following partition function accounts for all of the cases that are presented:

$$Q = \prod_{i}^{m}(1 + K_{a,i}[X]) + K_u\prod_{j}^{n}(1 + K_{b,j}[X]) \quad (1)$$

Q is the partition function, which is the sum of the statistical weights of all species in the system relative to the reference species, the native, unliganded protein. K_u is the intrinsic unfolding constant for the protein (i.e., in the absence of ligands). $K_{a,i}$ is the association constant for binding to the ith site of the native state (with m independent sites). $K_{b,j}$ is the association constant for binding to the jth site in the unfolded state (with n independent sites). [X] is the free ligand concentration. The association constants are defined for any independent site as follows.

$$K_u = \frac{[U]}{[N]}$$

$$K_a = \frac{[NX]}{[N][X]} \quad (2)$$

$$K_b = \frac{[UX]}{[U][X]}$$

The partition function for any of the cases shown in Scheme 1 can be obtained from eq 1 by setting to zero those association constants that do not apply to a given scheme. The temperature dependence of each binding constant is defined through the temperature dependence of the free energy:

$$\Delta G°(T) = \Delta H_r - T\Delta S_r + \Delta C_p\left[T - T_r - \ln\left(\frac{T}{T_r}\right)\right] \quad (3)$$

and

$$K(T) = e^{-(\Delta G°/RT)} \quad (4)$$

From the partition function, we can obtain the excess enthalpy for the system at any temperature (T) as follows (*7*):

$$\langle\Delta H\rangle = -R\frac{\partial \ln Q}{\partial\frac{1}{T}} \quad (5)$$

Further differentiation yields the excess heat capacity, which is the experimentally accessible quantity using differential scanning calorimetry (DSC):

$$\langle\Delta C_p\rangle = \frac{\partial\langle\Delta H\rangle}{\partial T} \quad (6)$$

The observed equilibrium constant is given by the intrinsic unfolding constant modified by the linked binding equilibria as follows (*3*):

$$K_{obs} = K_u\frac{\prod_{i}^{m}(1 + K_{a,i}[X])}{\prod_{j}^{n}(1 + K_{b,j}[X])} \quad (7)$$

The temperature at which K_{obs} is equal to 1 is the observed T_m. The observed enthalpy of unfolding is obtained as follows:

$$\Delta H_{u,obs} = -R\frac{\partial \ln K_{obs}}{\partial\frac{1}{T}} \quad (8)$$

The equations presented above do not consider the effects of a buffering species explicitly. This is valid for cases where proton linkage is not significant (i.e., there are no pK_a shifts upon binding). Further, the trends and relative behavior of the system will be largely unaffected by buffer when various ligands are being compared under the same conditions. However, if one is considering protons as ligands, the buffer needs to be considered and is treated as a pseudolinkage (*7*) as the buffer affects the free proton concentration and, therefore, the state of the system at every temperature.

The free ligand concentration can be calculated analytically for cases A and B in Scheme 1. In cases where multiple binding events and/or a buffer is included, mass and charge balance relationships are included to iteratively solve for the free ligand concentration.

METHODS

Simulation. Simulations were performed using Microsoft Excel 2000 and the included Visual Basic for Applications (VBA) for automating numerical solutions for the free ligand concentration at each temperature. The spreadsheet was set up to calculate all of the quantities described above at each

temperature in the range of 270−400 K using an increment of 0.05 K. Calculation of the relevant terms at each temperature requires the temperature dependence of all the terms in the equations to be defined. This is accomplished in the simulation by allowing the user to set the intrinsic energetics of ligand binding and buffer properties (enthalpy, entropy, and heat capacity changes) at a reference temperature for each binding event individually, along with the intrinsic unfolding energetics and the total protein, ligand, and buffer concentrations. In cases where an analytical expression cannot be obtained, calculation of the free ligand concentration was accomplished iteratively using Excel's GoalSeek function. This function iteratively solves for a free ligand concentration that makes the expression for the total buffer concentration equal to the user-defined total buffer concentration. The expression for the total buffer concentration is derived from the mass and charge balance relationships and includes terms for free ligand concentration, association constants, as well as the autoionization of water, and total protein, ligand, and buffer concentrations. The iteration was continued until the maximum difference between the calculated and desired buffer concentration was $\leq 1 \times 10^{-11}$.

RESULTS

From the models presented above, a variety of conditions can be investigated relatively quickly. The examples most relevant to drug screening and unfolding energetics are discussed here.

Screening for Drug Candidates. The case most relevant to drug screening procedures is unfolding in the presence of a single ligand which binds to the native state. Figure 1A shows the calculated excess heat capacity curves for Scheme 1A. In each case, the association constant at 25 °C is the same, but the enthalpy of binding is varied. When the enthalpy is positive, binding is entropically driven, and when the enthalpy of binding is negative, binding is enthalpically driven. Although the observed melting temperature (approximately the peak maximum of each excess heat capacity curve) is always increased when ligand binds to the native state, the magnitude of the increase is larger when the binding is entropically driven than when the binding is enthalpically driven, even though the binding constants at 25 °C are the same.

Figure 1A indicates that a given T_m is not unique to a given binding affinity. There is a range of binding affinities that can give rise to the observed shift in melting temperature. A large association constant with a favorable enthalpy can give rise to the same observed T_m shift as a weaker binding event with an unfavorable enthalpy. Figure 2 displays the combination of binding constants and enthalpies that give the same increase in melting temperature. As a specific example, consider that a T_m shift of 20 K could correspond to an association constant ranging from 1×10^3 to 1×10^8 for values of enthalpy from −100 to 100 kJ/mol.

For binding a single ligand to the unfolded state of the protein (Scheme 1B), a similar trend is observed. Rather than an increase, there is a decrease in the observed T_m because the unfolded state is now being stabilized by the interaction. Figure 1B shows the same trend observed in Figure 1A for a single ligand binding to the unfolded state of the protein.

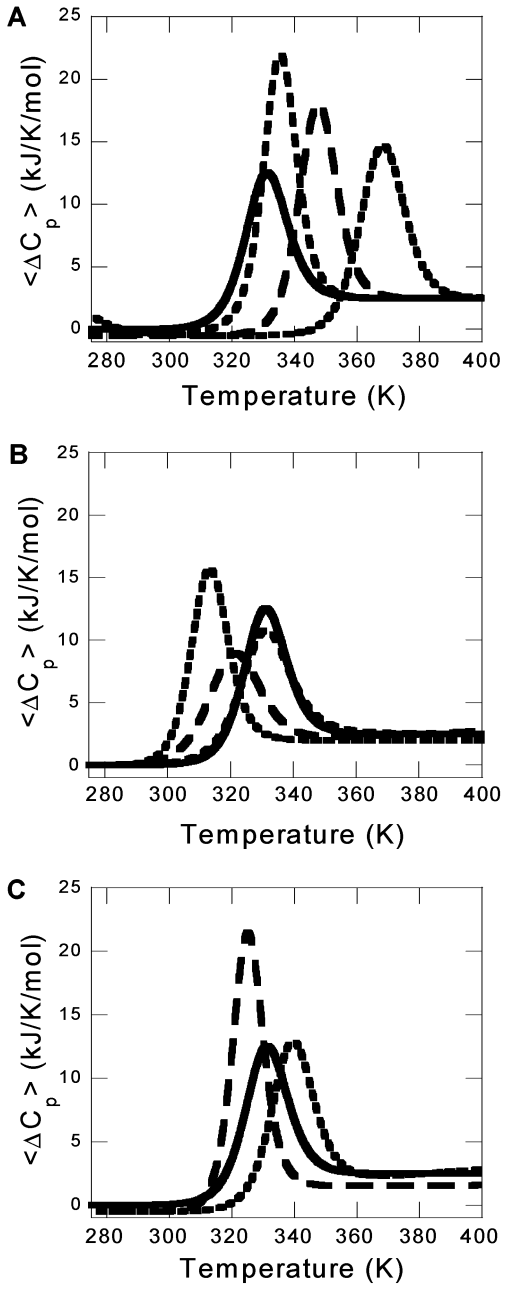

FIGURE 1: Simulated DSC curves for unfolding in the presence of a ligand. (A) Ligand binding to the native state (Scheme 1A), with varying enthalpies of binding. Simulation conditions are as follows: $\Delta H_u(T_o) = 200$ kJ/mol, $T_o = 330$ K, $\Delta C_{p,u} = 2.5$ kJ K^{-1} mol^{-1}, $K_a(298\text{ K}) = 1 \times 10^6$, ΔC_p for binding $= -0.5$ kJ K^{-1} mol^{-1}, $[\text{ligand}]_{tot} = 0.1$ mM, $[\text{protein}]_{tot} = 0.01$ mM, and $[\text{buffer}]_{tot} = 0.02$ mM. The solid curve is unfolding in the absence of ligand. Dashed curves from left to right correspond to $\Delta H_a(298\text{ K})$ values of −75, 0, and 75 kJ/mol, respectively. (B) Ligand binding to the denatured state (Scheme 1B), with varying enthalpies of binding. Simulation conditions are the same as for panel A except $K_a(298\text{ K}) = 1 \times 10^5$, and dashed curves from left to right correspond to $\Delta H_b(298\text{ K})$ values of 75, 0, and −75 kJ/mol, respectively. (C) Observed melting temperature shifts for ligand binding to both the native and unfolded states (Scheme 1C). Simulation conditions use the same intrinsic unfolding parameters as described above. The single binding to the native state occurs with the following parameters: $K_a(298\text{ K}) = 1 \times 10^8$, $\Delta H_a(298\text{ K}) = -50$ kJ/mol, and $\Delta C_p = -0.5$ kJ K^{-1} mol^{-1}. Five bindings to the unfolded state occur with a $K_b(298\text{ K})$ of 1×10^3 and a ΔC_p of −0.2 kJ K^{-1} mol^{-1}. From left to right, for each of the five sites, $\Delta H_b(298\text{ K}) =$ 10 and −10 kJ/mol.

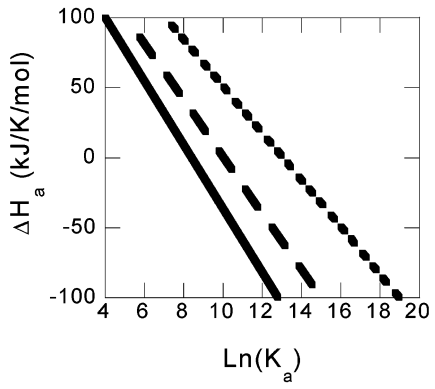

FIGURE 2: Range of association constants and enthalpies (at 298 K) of ligand interaction that can give rise to the same observed melting temperature shift. Lines indicate combinations of binding enthalpy and K_a that give the same shift in T_m. From left to right, the T_m shift is 5, 10, and 20 K. Simulation conditions are as follows: $T_o = 330$ K, $\Delta H_u(T_o) = 200$ kJ/mol, $\Delta C_{p,u} = 2.5$ kJ K^{-1} mol^{-1}, $[\text{protein}]_{tot} = 0.01$ mM, and $[\text{ligand}]_{tot} = 1$ mM.

Entropically driven binding results in a larger T_m shift away from the intrinsic T_m (i.e., the T_m in the absence of ligand) than enthalpically driven binding events, which tend to resist T_m shifts.

The competing effects of these two cases are demonstrated in Figure 1C where a single, tight binding site in the native state that is enthalpically driven (resisting a shift in T_m) can be masked by several weaker binding sites in the unfolded state of the protein that are entropically driven (enhancing an opposite T_m shift). In fact, the protein can be destabilized even though the ligand binds to the native state.

Heat Capacity Change upon Protein Unfolding. These observations apply to proton binding events as well. Scheme 1D shows the unfolding of a protein which has five ionizable acidic side chains. The side chains can have different proton affinities (i.e., pK_a's) in the native and unfolded states. As an example, we have used the experimentally determined pK_a values for the acidic side chains in a small protein, turkey ovomucoid third domain (*8*), and model values of aspartate and glutamate free in solution for the unfolded pK_a's (*9*) to look at unfolding behavior as a function of pH. Calculation of both the T_m and the enthalpy of unfolding at the T_m allows construction of plots of ΔH_m versus T_m. Experimentally, the slope of this plot is taken to be the $\Delta C_{p,u}$ for protein unfolding (*10*). Thus, we have a way to determine what we would expect experimentally for error in determining unfolding heat capacities.

Figure 3A shows the plots produced using energetics for glycine as the buffer for the pH range from 1.5 to 3.5, and acetate energetics for the pH range from 3.5 to 5.5. Since there is a change in proton affinity for each ionizable side chain between the native and unfolded protein, there must be a change in either the enthalpy of the association, the entropy of the association, or both. Figure 3A shows both extremes where the shift in pK_a's is entirely entropic or entirely enthalpic. The slope of the best fit line to these points is the observed heat capacity change for the unfolding transition, while the intrinsic $\Delta C_{p,u}$ is set at 2.5 kJ K^{-1} mol^{-1}. If all of the pK_a shifts are entropic in origin, the error is small with an estimate of 2.48 kJ K^{-1} mol^{-1}. However, if the pK_a shifts are enthalpic, the error is sizable, with an estimate of 2.84 kJ K^{-1} mol^{-1}.

Different buffers produce varying degrees of error. Figure 3B shows the same simulation performed using phosphate to buffer from pH 1.5 to 3.0. The error in this case is much more significant than that using glycine. Estimates of 2.59 and 2.93 kJ K^{-1} mol^{-1} are obtained for $\Delta C_{p,u}$ when the pK_a shifts are entropic and enthalpic, respectively. Fitting a line to phosphate alone (Figure 3C) estimates the heat capacity for unfolding to be 1.84 kJ K^{-1} mol^{-1} when the pK_a shifts are entropic and 2.43 kJ K^{-1} mol^{-1} when the pK_a shifts are enthalpic. This underscores the importance of investigating a wider pH range, and the proper buffer choice when performing DSC experiments and analyzing them quantitatively.

Others have reported results of simulations using various approximations (*1*, *4*−*6*). These approximations include the assumption that the free ligand concentration remains constant throughout the temperature range and that the effect of buffer on the transition is minimal. Figure 3D shows the case where there is no enthalpy contributed from a buffer and the free proton concentration is assumed to remain constant throughout the temperature range of the melt. Note the slight curvature that appears in this plot. Such data would estimate $\Delta C_{p,u}$ to be 2.6 and 2.8 kJ K^{-1} mol^{-1} for the entropic and enthalpic cases, respectively.

DISCUSSION

A recent report presents data with a new differential scanning calorimeter with higher throughput than traditional instruments (*11*). They demonstrate that it is possible to obtain very good data from this method. They are careful to state one can only really compare ligands by assuming that the ligands bind with similar enthalpies (without prior knowledge of their binding energetics). A number of studies, as well as unpublished work from our own lab, have shown that similar ligands can bind to their targets with significantly different enthalpies, while producing small effects on the overall binding free energy (*12*, *13*). Thus, it cannot be assumed that various ligands in a drug screen will bind with similar enthalpy. Fortunately, DSC can provide information about the binding enthalpies, which makes it a powerful technique. Other methods for monitoring unfolding, while able to detect the degree of unfolding and the change in melting temperature, are not sensitive to the heats of ligand binding and release; therefore, these methods require more caution when observed shifts in melting temperature are compared because it is unclear if the ligands bind with different enthalpies. Even using DSC, difficulty in discriminating between drug candidates can arise due to the need to extrapolate results to a common temperature (preferably a physiologically relevant temperature) to make meaningful comparisons. These extrapolations require accurate knowledge of the unfolding energetics. For this reason, an accurate determination of ΔC_p is required, hence the discussion on determining ΔC_p.

Screening for Drug Candidates. Through the cases presented here, it is demonstrated that the energetics of protein−ligand binding must be considered to accurately interpret shifts in the melting temperature of a target protein. When two different ligands are compared, one may bind with a lower affinity but be entropically driven, while the other may bind with a higher affinity and be enthalpically driven. For

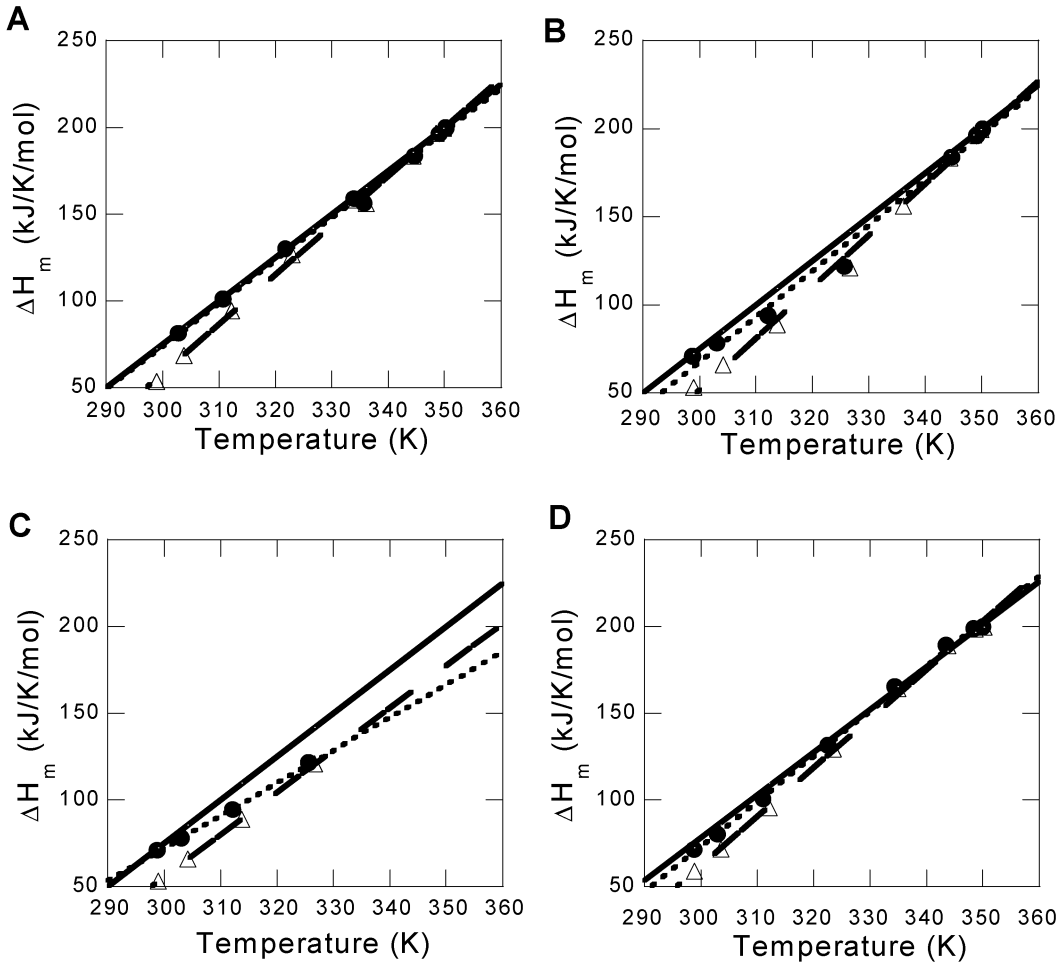

FIGURE 3: Simulated plots of unfolding enthalpy at the melting temperature vs melting temperature, produced by varying the pH at which the unfolding occurs. In each graph, filled circles are used for the case where the pK_a shifts are entirely entropic (best fit line shown as a dotted line), while the empty triangles show the case where all pK_a shifts are enthalpic (best fit line shown as long dashes). The slope of the solid line with no markers represents the intrinsic unfolding heat capacity of the protein. (A) Five pK_a changes where the native state pK_a's are those reported for the native state of the turkey ovomucoid third domain and the pK_a's for the unfolded protein are those reported for the amino acids free in solution. Glycine is used to buffer from pH 1.5 to 3.5, and acetate is used to buffer from pH 3.5 to 5.5. (B) Same as panel A except the buffer used from pH 1.5 to 3.0 is phosphate instead of glycine. (C) Plotting the pH range of 1.5−3 from panel B. (D) Plot generated for entropic pK_a shifts, assuming no enthalpy of ionization for the buffer, and a constant free proton concentration throughout the unfolding.

example, consider a hypothetical case according to Scheme 1A. At 25 °C, ligand 1 binds to a target with an association constant of 1×10^6, an enthalpy of −40 kJ/mol, and a heat capacity change of −500 J K^{-1} mol^{-1}, while ligand 2 binds with an association constant of 1×10^5, an enthalpy of 20 kJ/mol, and a heat capacity change of −500 J K^{-1} mol^{-1}. The binding constant for the protein−ligand interaction at the T_m is calculated as (*1*)

$$K_a(T_m) = \frac{e^{\{(-\Delta H^\circ/R)(1/T_m - 1/T_o) + (\Delta C_p/R)[\ln(T_m/T_o) + (T_o/T_m) - 1]\}} - 1}{[L]_{T_m}} \quad (9)$$

where $K_a(T_m)$ is the association constant for the ligand at the melting temperature of the protein, T_m is the melting temperature of the protein in the presence of ligand (360.3 and 365.85 K for ligands 1 and 2, respectively, in this example), T_o is the melting temperature of the protein in the absence of ligand (350 K), ΔH° and ΔC_p are the unfolding energetics of the protein in the absence of ligand (300 kJ/mol and 4 kJ K^{-1} mol^{-1}, respectively), and R is the gas constant. $[L]_{T_m}$ is the concentration of unbound ligand at the T_m (0.995 mM for both ligands, because we are under conditions where the ligand is in excess of the protein). Equation 9 gives K_a values for the first ligand of 2.2×10^4 and for the second ligand of 1.4×10^5. These calculated affinities need to be extrapolated to the same temperature to be compared directly, either to the same T_m or to a physiologically relevant temperature. If we choose to extrapolate to the T_m for ligand 1 to minimize the error introduced due to the extrapolation, then we conclude that ligand 2 binds with a higher affinity (1.5×10^5) than ligand 1. However, we know that if we were to extrapolate to 25 °C, ligand 1 in fact binds with a higher affinity. To properly extrapolate the data to another temperature, we need both the enthalpy and heat capacity changes associated with ligand binding which requires unfolding experiments using at least two different ligand concentrations.

Examination of the T_m shift alone would lead to the erroneous conclusion that the entropically driven binding event (ligand 2) is a better drug candidate. The ranges of association constants that can be obtained, depending on the

enthalpy of the interaction for a given T_m shift, are shown in Figure 2. These ranges underscore the importance of considering the full energetic profile of ligand binding and not simply the T_m shift as the important parameter. Even when the enthalpy for the binding reaction is small relative to the unfolding enthalpy (as is assumed in most treatments), significant effects on the observed T_m shift result.

If we consider cases where a decrease in T_m is observed, it is clear that caution must be exercised when quickly discounting potential drug candidates (see Figure 1C). Even when a decrease in the melting temperature is observed (reflecting denatured state binding), binding to the native state may be occurring. Assuming that binding must occur according to Scheme 1A could cause good drug candidates to be overlooked. Certainly, any physiologically relevant use of such a compound would be at lower temperatures where the ligand binding to the native state is, in fact, tight and enthalpically favorable. Although this is a somewhat extreme case, the point is still relevant to cases where the interaction of the ligand with the denatured state may be weak, but can still affect the observed T_m shift and the fitted binding constant. The full characterization requires that unfolding be conducted at several concentrations of the interacting ligand. This would allow a global fit of the data to determine all the relevant parameters for unfolding (T_o, ΔH_u, and $\Delta C_{p,u}$) as well as the energetics of ligand binding (ΔH_a, K_a, and ΔC_p).

Heat Capacity Change upon Protein Unfolding. Since the determination of protein−ligand interaction energetics from DSC requires an accurate determination of the heat capacity change upon unfolding for extrapolation, we have used these simulations to investigate potential errors with this parameter. Obtaining the heat capacity change for unfolding from a single DSC scan is generally unreliable, due to the difficulty in constructing baselines. Fortunately, the choice of a reasonable baseline does not affect the resulting determination of the unfolding enthalpy or the T_m.

The common approach to determining ΔC_p is to plot the unfolding enthalpy versus T_m over a range of pH values (see ref *10* and references therein). Using pH to perturb the melting temperature is represented as the binding of protons to both the native and denatured states of the protein (Scheme 1D). This allows us to simulate the pH dependence of the stability for a protein with known pK_a's. There are several features of this set of simulations to note. First, when a pK_a in the native state is different than the unfolded state pK_a, the shift can arise through changes in the enthalpy and/or entropy of the ionization. If the pK_a shift is purely entropic, the ionization of the side chain in the native state and denatured state occurs with the same enthalpy. Thus, we can try to choose a buffer that has the same ionization enthalpy as the side chains. With a matched buffer whenever a proton is picked up or released by the protein upon unfolding, the buffer releases or picks up a proton, respectively, and the heats cancel. In this way, there is no net enthalpic contribution to the observed unfolding transition, leaving us with contributions only from changes within the protein and its interaction with the solvent.

The situation is more complicated if the pK_a shifts are enthalpic. In this situation, the enthalpy of ionizing a side chain in the native state is different than the enthalpy of ionizing the unfolded state. Consequently, no "matching" buffer can be used since the ionization enthalpy differs for the folded and unfolded states. This results in a net contribution to the unfolding enthalpy.

We have used these simulations to demonstrate that the differences can be significant in determining $\Delta C_{p,u}$ as seen in Figure 3. Even though the ionization enthalpy of the buffer is small, and changes in the free proton concentration over the course of an unfolding experiment are considered small, significant effects on the determined $\Delta C_{p,u}$ can result. Assumptions about the effect of buffer enthalpy and free proton concentration have significant effects on the expected $\Delta C_{p,u}$. In this example, it is clear that these assumptions lead to estimates of $\Delta C_{p,u}$ that do not capture the intrinsic value even when the pK_a shifts are entropic. Also, poorly chosen buffers can significantly distort the determined values for $\Delta C_{p,u}$.

These simulations also underscore the need to further understand the origins of pK_a shifts that occur in proteins. It is not simply the pK_a shift itself that is important, but rather the underlying energetic profile that is essential to our understanding. It will be increasingly important to understand whether pK_a shifts are enthalpic or entropic in origin as instrumentation improves in sensitivity and we progress in our understanding of proteins. Without this understanding, the extent of the error associated with $\Delta C_{p,u}$ measurements is uncertain.

Concluding Remarks. The work presented here has demonstrated that caution must be taken in interpreting the effects of ligand binding on shifts in melting temperature. Accurate determination of the binding energetics at physiologically relevant temperatures requires multiple unfolding experiments if the binding energetics are not previously known. Fortunately, in the case of DSC, various binding modes (i.e., enthalpic or entropic) can, in principle, be detected. The situation may not be the same for other techniques where the heats of interaction are not measured and determination of binding energetics is more difficult. Complicating extrapolations of binding data to physiologically relevant temperatures are uncertainties that accompany the measurement of unfolding energetics. The work presented here makes it clear that a full understanding of the origins of pK_a shifts of ionizable groups also needs further investigation because of the important role that these pK_a shifts play in the observed stability of proteins. If the difference between pK_a's for an ionizable group in the native state versus the unfolded state arises from a shift in the enthalpy of the ionization, a significant error in the apparent heat capacity of unfolding can result. Additionally, poor buffer choices can add to errors in such measurements. We are currently undertaking studies monitoring unfolding of proteins with known pK_a's as a function of buffers with various ionization enthalpies in the hope that this will help to sort out some of these questions.

REFERENCES

1. Brandts, J. F., and Lin, L. N. (1990) *Biochemistry 29*, 6927−6940.
2. Lumry, R., and Biltonen, R. (1966) *Biopolymers 4*, 917−944.
3. Schellman, J. A. (1975) *Biopolymers 14*, 999−1018.
4. Straume, M., and Freire, E. (1992) *Anal. Biochem. 203*, 259−268.
5. Shrake, A., and Ross, P. D. (1992) *Biopolymers 32*, 925−940.

6. Robert, C. H., Colosimo, A., and Gill, S. J. (1989) *Biopolymers 28*, 1705−1729.
7. Wyman, J., and Gill, S. J. (1990) *Binding and Linkage: Functional Chemistry of Biological Macromolecules*, University Science Books, Mill Valley, CA.
8. Schaller, W., and Robertson, A. D. (1995) *Biochemistry 34*, 4714−4723.
9. Christensen, J. J., Hansen, L. D., and Izatt, R. M. (1976) *Handbook of Proton Ionization Heats*, John Wiley & Sons, New York.
10. Privalov, P. L. (1979) *Adv. Protein Chem. 33*, 167−241.
11. Plotnikov, V., Rochalski, A., Brandts, M., Brandts, J. F., Williston, S., Frasca, V., and Lin, L. N. (2002) *Assay Drug Dev. Technol. 1*, 83−90.
12. Breslauer, K. J., Remeta, D. P., Chou, W. Y., Ferrante, R., Curry, J., Zaunczkowski, D., Snyder, J. G., and Marky, L. A. (1987) *Proc. Natl. Acad. Sci. U.S.A. 84*, 8922−8926.
13. Luque, I., and Freire, E. (2002) *Proteins 49*, 181−190.

BI034212V